Tetrahedron Vol. 43, No. 17, pp. 3863 to 3874, 1987
Printed in Great Britain.

0040-4020/87 $3.00+.00

Stereoelectronic Effects on the Nucleophilic Addition of Phosphite to the Carbonyl Double Bond: Ab Initio Molecular Orbital Calculations on Reaction Surfaces and the α-Effect

Jen-Wen A. Chang†, Kazunari Taira†, Shigeyuki Urano†, and David G. Gorenstein‡*

Departments of Chemistry

†*University of Illinois at Chicago*

Chicago, Illinois 60680

and

‡*Purdue University*

W. Lafayette, Indiana 47907

(*Received in USA* 24 *November* 1986)

Abstract: Ab initio molecular orbital calculations have been carried out on adducts of trihydroxy phosphine, $P(OH)_3$, and formaldehyde, $H_2C=O$. Stationary points were located and a reaction surface calculated. One stationary point exists as a stable pentacovalent phosphorane, and the other as a 1,3-dipolar transition state. Calculations differing in the conformation about the P-OH bonds of the phosphite reveal that an antiperiplanar (app) lone pair on oxygen to the phosphorus lone pair (acyclic analogue) raises the energy of the molecule by 1.7 kcal/mol relative to a phosphite conformation with no app lone pairs to the phosphorus lone pair (bicyclic analogue). In the transition state, the relative energy between the two conformations reverses with the acyclic analogue transition state 5 kcal/mol lower energy than the bicyclic analogue transition states. The lower energy for the acyclic analogue in the transition state is attributed to the mixing of the app lone pairs on the oxygens of the phosphite mixing with the σ^* orbital of the newly formed bond between phosphorus and carbon. This kinetic stereoelectronic effect can explain why acyclic phosphites react much faster in nucleophilic reactions than bicyclic phosphites. This phenomenon suggests that the origin of the α-effect, the enhanced nucleophilicity of a base possessing a heteroatom with an adjacent unshared electron pair arises from the stereoelectronic effect.

INTRODUCTION

Phosphite as well as phosphate esters undergo marked changes in properties (basicity, nucleophilicity, rate of hydrolysis) upon inclusion of the phosphorus atom into a monocyclic or a bridgehead bicyclic system[1-15]. Thus, as shown in the following scheme, the bicyclic phosphite, 1, reacts much slower than acyclic phosphites in nucleophilic or biphilic reactions.

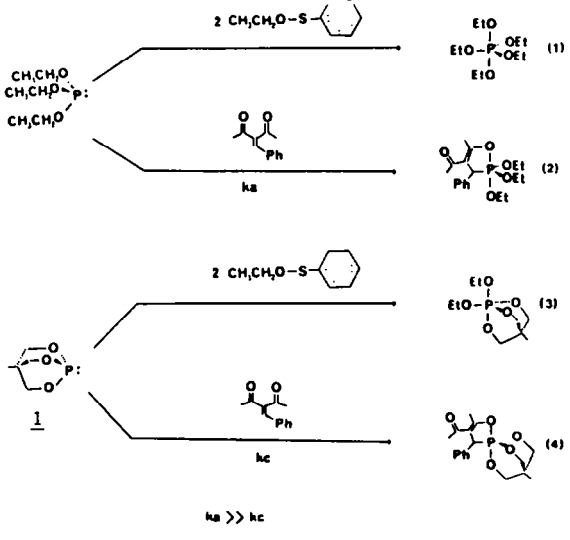

Our laboratory has suggested that stereoelectronic effects play an important role in these properties and that the alpha effect, the enhanced nucleophilicity of a base possessing a heteroatom with an adjacent unshared electronic pair is another manifestation of the stereoelectronic effect.

A stereoelectronic effect provides the most satisfying explanation for the poor nucleophilicity[1,11] of the bicyclic

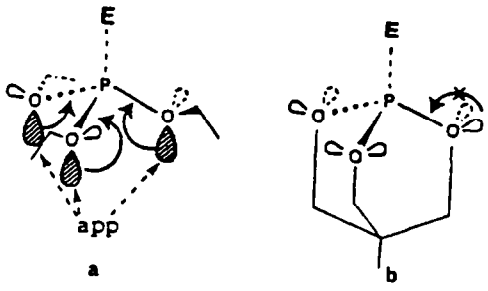

Figure 1 Nucleophilic attack by phosphorus nucleophile with(a) or without(b) app lone pair electron.

phosphite, 1. In the case of triethyl phosphite, assuming free rotation about the P-O bond (Figure 1a), a maximum of three lone-pair orbitals on the oxygens may be oriented antiperiplanar (app) to the newly formed phosphorus-electrophile (P-E) bond. However, no comparable orientation of the oxygen lone pair is possible for the bicyclic phosphite because of ring constraints (all lone pair are locked gauche to the incipient P-E bond; Figure 1b). This kinetic stereoelectronic effect is believed to arise from the stabilization of the transition state through effective overlap and mixing (in a trans/antiperiplanar orientation) of the lone pair orbital, n, with the antibonding P-X orbital, σ^*_{P-X}[11-17].

$$(RO)_3P + X\text{-}Y \rightarrow (RO)_3P^+\text{-}X + Y^-$$

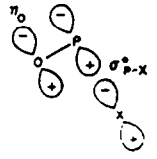

Because n-σ^*_{P-X} mixing in the acyclic phosphite is much greater than mixing of the O-C σ-bond and σ^*_{P-E} in the bicyclic phosphite[12], the energy of the acyclic transition state can be stereoelectronically significantly stabilized relative to that of the bicyclic transition state.

We report a theoretical analysis of the carbonyl addition reaction of acyclic and bicyclic phosphites. Formaldehyde was chosen as the electrophile and trihydroxy phosphine (or phosphite, $:P(OH)_3$) as the nucleophile.

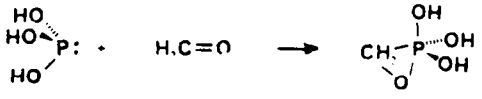

Although this theoretical reaction will be shown to yield a highly unusual three- membered ring phosphorane intermediate and transition states, evidence for such structures has recently been proposed in the rearrangement reaction.[18]

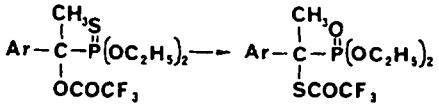

The three-membered ring phosphorane is quite likely an intermediate in this reaction:

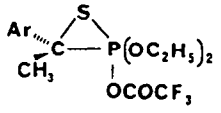

Reactions surfaces have been calculated for different orientations about the P-OH bond in trihydroxy phosphine representing the geometries of bicyclic and various acyclic phosphites. Most importantly, during the cleavage of the

P-C bond in the stable pentacovalent phosphorane adduct $(HO)_3P\ H_2C{=}O$, transition states are clearly established for both geometries and the acyclic transition state is found to be 5 kcal/mol lower energy than the bicyclic transition state. These results support our emphasis that the kinetic stereoelectronic effect and the α-effect are largely transition state phenomena.[12]

METHOD OF CALCULATION

The SCF LCAO-MO *ab initio* calculations utilized the Gaussian 80 series of programs[19]. All stationary points were located with either Murtagh-Sargent[20] or Berny optimization methods.[19] First, full geometry optimization in each phosphite conformation was done for all local minima and transition state structures using STO-3G basis functions diagonalizing the analytically determined matrix of force constants. Single-point calculations on the STO-3G optimized geometries failed at the split valence 3-21G level. Thus, a full geometry optimization was again carried out on the 3-21G basis set, starting from the geometry obtained at the STO-3G level. Additional results are reported base upon 6-21G and various other basis sets with and without polarization functions by using single-point calculations at STO-3G and 3-21G optimized geometry. ORTEP plots[21] were generated from the coordinates of the optimized structures.

All calculations were carried out on an IBM 3081 computer.

RESULTS

1 Pentacovalent Intermediates

Four different conformations of the ground state pentacovalent phosphoranes formed by addition of phosphite to formaldehyde were geometry optimized using the geometry optimization routine of Gaussian 80 with STO-3G and 3-21G basis functions. The optimized geometries are shown in Table 1.

The stationary points representing the phosphorane intermediates A1, C1, A2, and C2 may be described as distorted trigonal bipyramids (tbp). Because of the constraints imposed by the three-membered PC_8O_9 ring, the normal 90° axial/equatorial ligand bond angle in a tbp is reduced to 60-70° in the four phosphoranes. The three "equatorial" sites in A1 and C1 are C_8, O_4 and O_5 and the two axial sites are O_2 and O_8 (note $<O_2PO_8$ is 159° and 164° in C1 and A1 respectively rather than the expected 180° in an undistorted tbp). In A2 and C2, C_8 and O_2 are

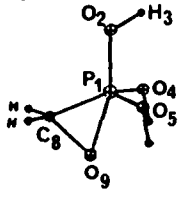

Table I Optimized geometries and energies of stable phosphoranes

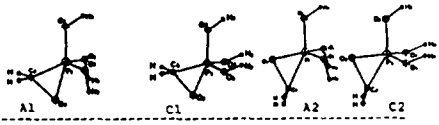

Parameter[a]	A1[b]	A1[c]	C1[b]	C1[c]	A2[c]	C2[c]
P_1-O_2	1.681	1.681	1.702	1.686	1.641	1.672
O_2-H_3	0.987	0.965	0.990	0.965	0.964	0.964
P_1-O_4	1.672	1.641	1.688	1.644	1.642	1.651
O_4-H_6	0.987	0.967	0.990	0.964	0.964	0.964
P_1-O_9	1.714	1.777	1.695	1.709	1.628	1.645
P_1-C_8	1.752	1.759	1.752	1.763	1.895	1.810
C_8-O_9	1.491	1.521	1.492	1.529	1.571	1.567
C_8-H	1.087	1.074	1.087	1.073	1.075	1.077
$<P_1O_2H_3$	107.41	119.92	110.24	125.28	119.65	123.92
$<O_2P_1O_4$	93.27	95.67	95.30	96.69	94.70	96.90
$<P_1O_4H_6$	106.26	115.04	107.17	123.50	118.72	124.73
$<O_2P_1O_9$	164.36	162.76	159.41	156.39	98.82	93.04
$<P_1O_9C_8$	62.61	63.91	62.40	65.73	72.57	68.54
$<O_9C_8H$	115.65	114.49	115.83	114.47	109.61	111.56
$<C_8P_1O_9$	50.94	50.97	51.26	52.21	52.37	53.68
$\tau O_4P_1O_2H_3$	58.44	57.15	60.09	57.35	57.13	56.71
$\tau O_2P_1O_4H_6$[d]	180.00	180.00	60.00	60.0	180.00	60.00
$\tau O_9P_1O_2H_3$[d]	180.00	180.00	180.00	180.0	180.00	180.00
$\tau C_8O_9P_1O_2$[d]	0.00	0.00	0.00	0.00	180.00	180.00
Total Energy	-672.4293	-677.2968	-672.4111	-677.2574	-677.2781	-677.2545

a. All units in Angstroms, Degrees and Hartrees.
b. Geometry optimized with STO-3G basis functions.
c. Geometry optimized with 3-21G basis functions.
d. Fixed conformations.

Table II Transition state optimized geometry and the reaction coordinate eigenvalue of the quadratic force constant matrix for acyclic (A-TS) and bicyclic (C-TS) transition states.[a]

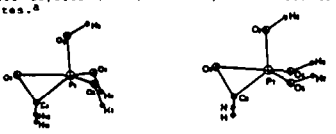

Internal Coordinate[b]	A-TS Geometry	A-TS Eigenvector	C-TS Geometry	C-TS Eigenvector
P_1-O_2	1.616	0.031	1.638	0.064
O_2-H_3	0.970	0.011	0.968	0.001
P_1-O_4	1.649	-0.018	1.644	0.009
O_4-H_6	0.965	-0.011	0.965	-0.001
P_1-O_9	2.202	-0.883	2.158	-0.884
P_1-C_8	1.816	c	1.792	c
C_8-O_9	1.427	0.352	1.442	0.363
C_8-H	1.088	-0.042	1.085	-0.014
$<P_1O_2H_3$	115.65	-0.016	120.17	-0.015
$<O_2P_1O_4$	97.54	-0.038	101.90	-0.084
$<P_1O_4H_6$	121.98	-0.054	127.57	-0.013
$<O_2P_1O_9$	84.04	0.211	82.47	0.196
$<P_1O_9C_8$	55.18	0.043	55.48	0.162
$<O_2P_1C_8$	124.25	c	124.01	c
$<P_1C_8O_9$	84.33	c	82.98	c
$<O_9C_8H$	118.56	-0.163	118.62	-0.097
$\tau O_4P_1O_2H_3$	53.79	0.043	55.49	0.013
$\tau O_2P_1O_4H_6$	180.00	d	60.00	d
$\tau O_9P_1O_2H_3$	180.00	d	180.00	d
$\tau C_8O_9P_1O_2$	180.00	d	180.00	d
Total energy	-677.2211		-677.2130	

a. Geometry optimized by 3-21G
b. All units in Angstroms, Degrees and Hartrees
c. Not a parameter in the Z-matrix
d. Fixed parameters in the Z-matrix

in the axial positions.

The relative energies (Table 1) of A1/A2 as well as C1/C2 at the 3-21G level of calculation are in agreement with the "preference rules" for stable phosphoranes[7,22-27]. The more polar atom (oxygen atom in the three-membered ring) preferentially occupies the axial position and the less polar atom (carbon atom in the three-membered ring) occupies the equatorial position. Thus A1 is 11.7 kcal/mol more stable than C2.

The stable pentacovalent phosphoranes A1 and C1 differ in conformation about the equatorial P-OH bonds. Relative to the endocyclic apical P-O_8 bond, there are two antiperiplanar (app) lone pairs on the equatorial oxygens in A1 and none in C1. Relative to the exocyclic apical P-O_2 bond, there are no app lone pairs on the equatorial oxygens in A1 and two in C1.

The stereoelectronic effect is considered to arise from the mixing of a lone pair orbital with the antibonding σ^* orbital of an adjacent polar bond. In terms of a simple resonance picture for the stereoelectronic effect stabilization of the structure is thought to derive from an anomeric type. double bond-no bond resonance contribution.[11-17]

The bond opposite to the app lone pair has some no-bond resonance character and the bond containing an app lone pair has some double-bond character. The stereoelectronic effect will thus lead to lengthening of the polar bond app to the oxygen lone pairs, as confirmed by the results shown in Table 1. The endocyclic apical P-O_9 bond in A1 (1.777 Å; 3-21G basis set) is longer than the endocyclic apical P-O_8 bond in C1 (1.709 Å). However, the exocyclic apical P-O_2 in A1 (1.681 Å) is shorter than the exocyclic apical P-O_2 in C1 (1.686 Å). Based upon the same stereoelectronic argument, we expect that the apical P-C bond in A2 will be longer than that in C2. Also the exocyclic apical P-O bond in A2 will be shorter than that in C2. The results from Table 1 (the P-C bond is 1.895 Å in A2 and 1.810 Å in C2; the P-O bond is 1.641 Åin A2 and 1.672 Å in C2) are consistent with the prediction of the stereoelectronic effect.

Transition State Search

The search for the transition states for the addition of phosphite to formaldehyde were actually initiated by studying the reaction surface for breakdown of the metastable phosphorane intermediates A1/C1 and A2/C2. Four possibilities were considered:

- a) Initial P-C bond stretch of the phosphoranes with carbon in the equatorial position of the trigonal bipyramid (A1/C1).
- b) Initial P-O bond stretch of A1/C1.
- c) Initial P-O bond stretch of the higher energy phosphoranes with carbon in the apical position (A2/C2).
- d) Initial P-C bond stretch of A2/C2.

Search a

As we stretch the equatorial P-C bond of the distorted phosphoranes A1 and C1, we searched for the saddle point using the Gaussian 80 geometry optimization routines and a STO-3G basis set. Without a major relaxation of the other geometric coordinates (particularly the O-H bond distance, see below) no transition state was located. Indeed continued stretching of the P-C bond did not lead to the expected formaldehyde and phosphite products but rather surprisingly to methylene carbene (singlet) and phosphoric acid (H_3PO_4).

Allowing all of the geometry to relax in this search for a transition state involving stretching of the P-C bond in A1 and C1 we did locate a transition state. While a transition state was found, as indicated by a single negative quadratic force constant, analysis of the eigenvector of this transition state shows that it will decompose to methyl phosphate. This reaction path may be viewed as heterocyclic P-C bond cleavage to yield a carbanion/phosphonium zwitterion followed by subsequent intramolecular proton migration. Replacement of this proton by an alkyl group would presumably eliminate this pathway.

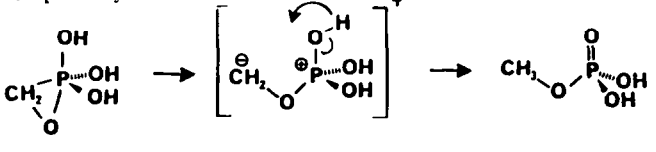

Search b

Unfortunately, by stretching the apical endocyclic P-O bond of conformation A1 and C1, which is more in keeping with the expected greater lability of the apical bond vs. the equatorial bond of trigonal bipyramid intermediates[7,28-38], no transition state was located. However, further search of the reaction surface suggested that the phosphorane decomposed to α-hydroxy phosphonate with initial cleavage of the P-O bond and subsequent proton migration.

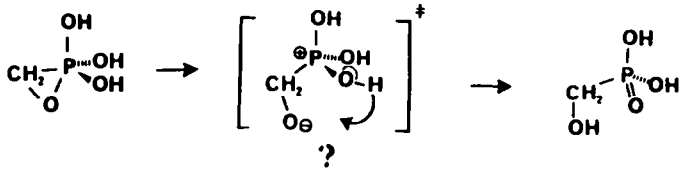

For decomposition of phosphoranes A1 and C1, both initial equatorial and axial bond scission pathways form a compound with a phosphorus-oxygen double bond. This is consistent with the strong oxygen affinity of phosphorus which can be seen in many organophosphorus reactions where formation of the very strong P=O double bond is a major driving force.[39]

Search c

By stretching the *equatorial* endocyclic P-O bond of phosphoranes A2 and C2 with the carbon apical we were able to locate the saddle points for the pathway yielding phosphite and formaldehyde. Table 2 shows the optimized geometry of the transition states and the eigenvectors of the single negative eigenvalue of the quadratic force constant matrix corresponding to the reaction coordinate. If we describe this eigenvector in terms of the internal coordinate motion representing the reaction coordinate, we can see that this reaction path represents the concerted addition of $P(OH)_3$ to $H_2C=O$ to yield the phosphorane.

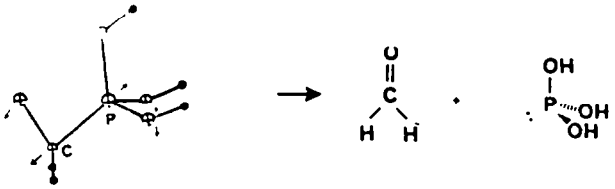

C-TS

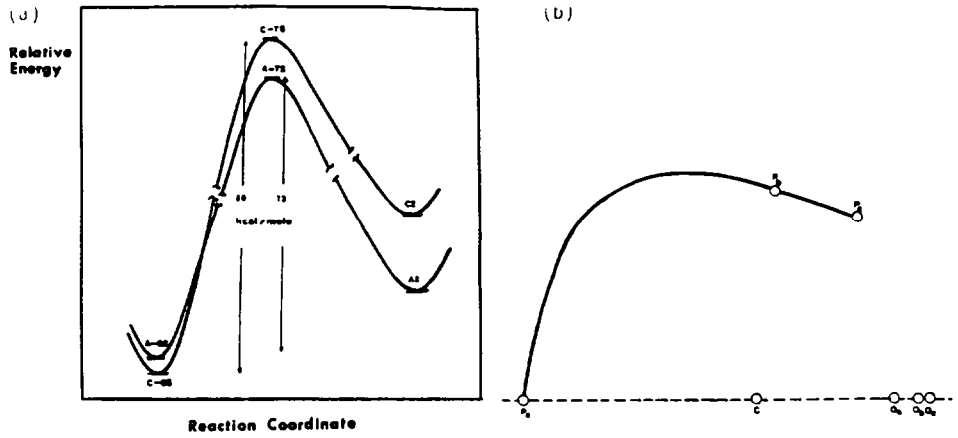

Figure 2 The relative energy diagram (a) and trajectory plot (b) for the addition reaction of phosphite and formaldehyde.

Search d

Finally, we searched for another saddle point using the Gaussian 80 geometry optimization routine by stretching the axial endocyclic P-C bond of phosphoranes A2 and C2. No transition state was located.

DISCUSSION

Ground State Stereoelectronic Effects in Phosphites

Shown in Table 3 are the relative energies and optimized geometries for different conformations of phosphites (representing acyclic and bicyclic analogs).

The results are basically consistent with the ground state anomeric or stereoelectronic effect[17]. In general, it is energetically more favorable to have a conformation about the P-O bond which allows an oxygen lone pair to be trans/antiperiplanar (app) to an adjacent polar bond (P-OH). This ground state stereoelectronic effect is presumed to arise from the orbital interaction of the oxygen lone pair orbital, n, with the adjacent antibonding orbital, σ_{P-O}. This two electron interaction of these two orbitals is stabilizing[12,28-32,40]. In contrast, it is destabilizing to have an oxygen lone pair orbital app to the phosphorus lone pair orbital[12]. This is a four-electron, lone pair-lone pair interaction which is overall destabilizing[12,40]. From Table 3, the bicyclic analog C-GS is 1.6 kcal/mol more stable (with 3-21G basis set) than the acyclic analog A- GS. It should be noted that the relative energies of A-GS and C-GS depend on the choice of different basis set (see additional discussion below). Apparently the various orbital stabilization and destabilization interaction[12] energies approximately cancel each other, and the overall energy is modestly sensitive to basis set quality.

Transition State Stereoelectronic Effect

As shown in Table 2 the acyclic analog transition state A-TS is 5 kcal/mol lower energy than the bicyclic analog transition state C-TS. This is consistent with the stereoelectronic effect since the oxygen lone pair electrons are app to the P-E scissile bond and effective mixing with antibonding σ_{P-E} stabilizes this transition state[12]. Figure 1 clearly shows that the acyclic analog A-TS has two lone pair electrons app to the newly forming P-E bond and bicyclic analog C-TS has none.

Figure 2 shows the reaction trajectory and relative energy diagram for the addition of phosphite to formaldehyde.

Table III Optimized Geometries of Phosphites[a]

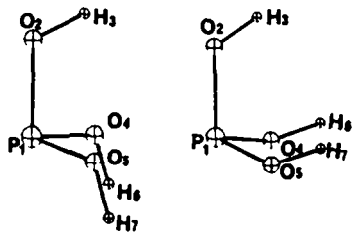

Internal coordinate[b]	A-GS Acyclic analogue	C-GS Bicyclic analogue
P_1-O_2	1.646	1.667
O_2-H_3	0.970	0.97
P_1-O_4	1.679	1.669
O_4-H_6	0.964	0.967
$\angle P_1O_2H_3$	116.81	123.95
$\angle O_2P_1O_4$	96.25	100.66
$\angle P_1O_4H_6$	120.22	124.23
$\angle O_4P_1O_2H_3$	50.40	51.19
$\angle O_2P_1O_4H_6$	180.00	60.00
Total energy in Hartrees	-564.11365	-564.115861
Relative energy in kcal/mol	0.00	-1.69[a] 1.61[c]

a. Geometries optimized with 3-21G basis set.
b. Units in Angstroms and Degrees
c. STO-3G Basis set (from ref. 6b).

Table IV. Population Analyses and Atomic Charges of Transition States (STO-3G* Basis Set)

	A-TS	C-TS
P_1-O_9	0.147	0.174
P_1-C_8	0.731	0.743
P_1-O_2	0.747	0.715
P_1-O_4	0.700	0.711
O_2-H_3	0.537	0.536
O_4-H_6	0.553	0.546
C_8-O_9	0.494	0.475
C_8-H_{10}	0.746	0.751
P_1	0.81	0.83
C_8	-0.09	-0.09
O_9	-0.45	-0.43
O_2	-0.35	-0.37
O_4, O_5	-0.39	-0.40
H_3,	0.27	0.25
H_6, H_7	0.26	0.25
H_{10}, H_{11}	0.04	0.05

As expected[41-43] the phosphite approaches the carbonyl double bond from above the plane of the formaldehyde. Burgi, et al.[41,42] and Baldwin, et al.[43] have analyzed the trajectories for nucleophilic attack on π-systems. For the first-row element nucleophile, the approach angle θ appears to be 70° (nucleophile-C-O bond angle 120°). Liotta, et al.[44] have shown that second-row nucleophiles, in contrast to first-row nucleophiles, have reaction trajectories with larger approach angles. Our calculations indicate that the trajectory approach angle θ is 95.7° (A-TS) and 97.0° (C-TS). As suggested by Liotta, et al.[44] this may partially be ascribed to the ability of these nucleophiles to participate in 3d back-bonding.

The calculated activation energies for the reactions of bicyclic and acyclic phosphites with formaldehyde are 80 kcal/mol and 73 kcal/mol, respectively. Thus the activation energy for the acyclic analog is 7 kcal/mol lower energy than the bicyclic analog activation energy. This activation energy difference can explain why the bicyclic phosphite 1 shows such poor nucleophilicity relative to acyclic phosphites in reactions involving the formation of phosphoranes.[11]

The only transition state that we could locate on the reaction hypersurface for the breakdown of the cyclic pentacovalent intermediate to yield phosphite plus formaldehyde originates from the higher energy phosphoranes with the P-C bond apical (A2, C2) rather than equatorial (A1, C1) (see the following section). This rather suprising result is actually totally in keeping with currently accepted reaction theory of pentacovalent phosphoranes[7] and the reaction path for nucleohilic addition to the carbonyl bond.[41-43] The calculated structures C-TS and A-TS represent early transition states along the forward reaction pathway forming the pentacovalent intermediates. Translation of the P-C bond largely describes the reaction coordinate and as discussed above the preferred trajectory is attack of the nucleophile from above the plane of the carbonyl double bond closest to the carbonyl carbon (approach angle 96-97°). Based upon the atomic charges and overlap populations (Table 4), the transition state is best described as a 1,3-dipolar species rather than a neutral phosphorane.

Thus P-O bond formation is not concerted with P-C bond formation. This 1,3- dipolar transition state, however, has characteristics of the phosphorane intermediate with an apical P-C bond which, of course, is formed at a later stage along the reaction coordinate. As would be expected, translation of the P-C bond in the phosphorane is favored for the longer apical bond and not for the equatorial "bond" of the pseudo trigonal bipyramid:

Table V. Calculated Energies for Cyclic (C) and Acyclic (A) Ground States (GS), Intermediates, Transition States (TS) Basis Sets/Energy (in-Hartrees)

Structure	STO-3G[a] Optimized	3-21G[b] Optimized	STO-3G[c] + d(P,O,C)	STO-3G[d] + d(P,O,C)	3-21G[e] + d(P)	3-21G[f] + d(P)	STO-3G[g]
C1	672.4111	677.2574	672.8575	672.8379	677.3987	677.2911	672.7350
C2	672.4086	677.2545	672.8651	672.8424	677.3987	677.2898	672.7399
A1	672.4363	677.2968	672.8868	672.8728	677.4379	677.3303	672.7712
A2	672.4263	677.2781	672.8916	672.8764	677.4254	677.3139	672.7731
C-TS	672.3422	677.2130	672.7428	672.7292	N.C.[h]	677.2390	672.6162
A-TS	672.3535	677.2211	672.7585	672.7445	N.C.[h]	N.C.[h]	672.6294
C-GS	560.1706	564.1159	560.4109	560.3913	564.1966	564.1335	560.3370
A-GS	560.1739	564.1132	560.4111	560.4004	564.1961	564.1301	560.3442
H_2CO	112.3543	113.2218	112.4195	112.4199	113.2218	113.2218	112.3543

(a) Standard STO-3G basis set, optimized geometry.
(b) Standard 3-21G basis set, optimized geometry.
(c) STO-3G plus standard d-functions on phosphorus, carbon and oxygen. Using (a) geometry.
(d) Same as (c). Using (b) geometry.
(e) 3-21G plus 3d function on phosphorus only, with scale factor 1.00.
(f) Same as (e) with scale factor 2.30. both (e) and (f) using geometry from (b).
(g) Standard STO-3G* basis set (polarization on P only) using geometry from (b).
(h) Did not converge.

Since it is an early (viewed in the forward direction) transition state with little P-O formation, the methylene is required to be in the axial position. Collapse of the 1,3-dipolar transition state (forming the P-O bond) thus yields the metastable phosphorane with the carbon atom in the apical position. Presumably if the transition state in the forward direction was "late" (defining the reaction coordinate now by the translation of the P-O bond during collapse of the 1,3- dipolar species) then we might expect that the transition state would have the carbonyl oxygen in the apical position:

Predicted favored late transition state (not observed)

These calculations have lead to the reaction mechanism for formation and breakdown of pentacovalent phosphoranes. Our calculations would suggest that the actual pathway, for example, for phosphite addition to an α,β-unsaturated diketone (reaction 2/4 in the introduction) would be the following:

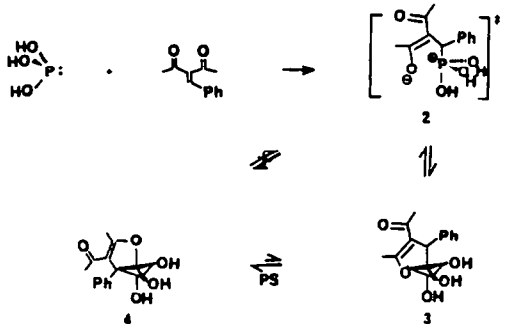

In the forward direction for formation of the phosphorane, with P-C bond formation rate limiting (as suggested experimentally[26,27]) the carbon must go into the "apical" position of 2. The collapse of the 1,3-dipolar species yields the high energy pseudorotamer 3. Pseudorotation will then provide the more stable phosphorane 4. By microscopic reversibility in the reverse direction, breakdown of the phosphorane apparently cannot proceed directly from 4, but rather from 3. The initial stage of the reaction coordinate will involve cleavage of the P-O bond in 3 from an equatorial postion followed by rate limiting cleavage of the P-C bond from the pseudo apical position in 2. Of course if the 1,3-dipolar species were a metastable intermediate rather than a transition state these predictions would be invalid (in fact evidence supports the intermediacy of 2[26,27]). However, at least from our calculation the 1,3-dipolar species is not a metastable local minimum.

Basis Function Dependence

Most of the calculations used complete geometry optimization with the STO-3G and 3-21G basis sets. As shown in Table 5 several different basis sets were also investigated. As would be expected[33-38], inclusion of d atomic orbital on phosphorus (keeping a single scale factor for all five d components) lowered the calculated energies of the structures. In some instances d-polarization functions were added to carbon and oxygen as well as using geometries optimized with STO-3G or 3-21G basis sets.

Comparison of three different basis sets - minimal basis function (STO-3G), split valence function (3-21G) and minimal basis plus d function for second row elements (STO-3G*) - indicated as expected that calculations with more extended basis functions gave more negative total energies. However, it is important to examine how *relative* energies vary with basis functions. Table 6 shows the calculated activation energy for reaction of acyclic and bicyclic phosphites using STO-3G, 3-21G and STO-3G* basis functions.

It has been shown that d orbitals play an important role in the accurate description of some properties of second-row molecules. Pople et al.[45] have demonstrated the addition of d functions results in a large increase in the binding energy, most dramatically for the hypervalent molecules. For normal-valence molecules, the increase in binding energy with the addition of d orbitals averages about 42 kcal/mol while that for the hypervalent molecules averages 235 kcal/mol.

Table 6 Calculated activation energies, ΔE^{I} utilizing different basis functions

	STO-3G[a]	3-21G[a]	STO-3G*[a]
Bicyclic $\Delta E^{\ddagger}$	114.65	78.25	47.50
Acyclic $\Delta E^{\ddagger}$	109.63	71.76	43.36
$\Delta\Delta E^{I}$	5.02	6.49	4.14

[a] kcal/mol

This analysis can be used to explain the difference in activation energies calculated with either STO-3G or STO-3G basis sets. The total energies of phosphites like the other normal-valence molecules are not affected greatly by the addition of d orbitals in the basis set. On the other hand, the transition states are similar to hypervalent molecules, and hence the addition of d orbitals dramatically lower the total energies of transition states which leads to the smaller activation energy in the STO-3G* level calculation.

However, we are not interested in the activation energies themselves but the activation energy *differences* between acyclic and bicyclic phosphites. These differences give a measure of the kinetic stereoelectronic effect. Table 6 also shows that the kinetic stereoelectronic effect ($\Delta\Delta E^{\ddagger} \sim 4.1$-6.5 kcal/mole) is essentially independent of basis function and consistent with the conclusions discussed earlier for the 3-21G geometry opimized structures. Recall that acyclic and bicyclic ground states and acyclic and bicyclic transition states differ only in conformation about the P-O bonds. Hence overall changes in energies resulting from basis set differences largely cancel, leaving only the conformational effects.

α-Effect

The α-effect, the enhanced reactivity of nucleophiles possessing a pair of electrons α to the nucleophilic atom, can be viewed as a stereoelectronic effect. Although numerous explanations have been provided for the "α-effect" (see references 46-48 and the references therein), one explanation that comes closest to the stereoelectronic orbital interaction picture is the one developed by Hudson[49,50] and Klopman[51]. Lone pair-lone pair orbital mixing (such as oxygen and phosphorus lone pairs in phosphites) will raise the energy of the HOMO and mixing with the lowest unoccupied molecular orbital (LUMO) will be enhanced. The major emphasis in these MO α-effect theories has been lone pair-lone pair interaction[49,50] rather than our stereoelectronic interpretation of transition state magnification of adjacent lone pair-σ^* interactions[11-13]. Indeed, as pointed out by Heaton[52] these "ground-state destabilization" arguments do not accord with the calculated and actual HOMO energies. His ab initio MO calculations instead emphasize the importance of the antibonding characteristics and higher polarizability of the α- effect HOMOs. All of these studies (including Heaton's) suffer from their emphasis on ground state properties of α-effect nucleophiles. As we have emphasized, the stereoelectronic effect (and likely the α-effect) is largely a transition-state phenomenon[11-15,28-32]. Significant mixing of n and σ^* is possible only in the transition state. It is this specific lowering of the transition state energy by α-effect lone pair electrons that presumably is responsible for a significant fraction of the enhanced reactivity of these α-effect nucleophiles.

Singlet Carbene Addition to P=O Double Bond

In our search of the reaction hypersurface we also considered the P-C bond- stretch reaction pathway involving C1 and A1 (search a). The minimum energy path as a function of this P-C distance (the rest of the geometrical degrees of freedom were optimized) also shows some very interesting results. As the P-C bond is stretched the C-O bond also stretches. Surprisingly, it did not lead to formation of formaldehyde plus phosphite but rather to singlet carbene ($:CH_2$) and phosphoric acid (H_3PO_4).

Because this pathway forms a highly unstable singlet carbene, the transition state was not located (in addition we are grossly oversimplifying the reaction surface by allowing only a singlet state to represent the carbene). Instead at variable P-C distances (defined as the reaction coordinate) the rest of the geometry was optimized. Figure 3 shows the calculated minimum energy reaction coordinate as a function of P-C bond length for the decomposition of the bicyclic (C1) and the acyclic (A1) phosphoranes. It is most important that the energy difference between the acyclic and the bicyclic geometries reaches a maximum at a P-C distance of ca. 2.45 Å(Figure 4) which is very close to the "transition state" P-C bond distance (Figure 3). The lower energy acyclic conformation has oxygen lone pairs app

to the translating P-C bond. Thus, at the P-C bond distance of 2.45 Å, the acyclic conformation is 19.6 kcal/mol lower energy than the bicyclic conformer.

Based on one-electron molecular orbital theory, the two-electron stabilization[40] resulting from the interaction of a doubly occupied MO (ξ) with a vacant nondegenerate MO (σ') may be approximated as being inversely proportional to the energy separation $\Delta E_{\xi\sigma'}$ of the two MO's and directly proportional to the square of their overlap, $S^2_{\xi\sigma'}$:

$$SE(\xi,\sigma') \propto \frac{S^2_{\xi\sigma'}}{\Delta E_{\xi\sigma'}}$$

Hence, the stereoelectronic effect provides the greatest stabilization energy at a P-C bond distance which provides the greatest $n_0 \leftrightarrow \sigma'$ (HOMO/LUMO) mixing. At very long P-C bond distances, overlap ($S_{\xi\sigma'}$) will also be negligible because the σ' orbital of the stable intermediate will be higher energy. Only at an intermediate distance (~2.5 Å) is a compromise reached where overlap is still sufficiently good and the energy difference still sufficiently small, to provide proper stereoelectronic stabilization of the structure. This will generally occur at the transition state.

These stereoelectronic consideration can rationalize the resistance to alkylation of the bicyclic phosphate observed in this lab and others[11].

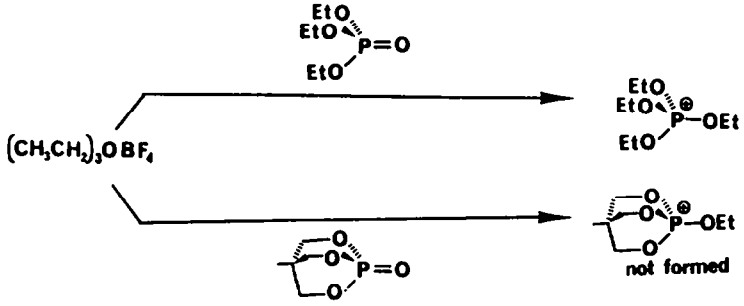

In the present calculation carbene is the electrophile and both the acyclic and the bicyclic geometries of $(HO)_3P{=}O$

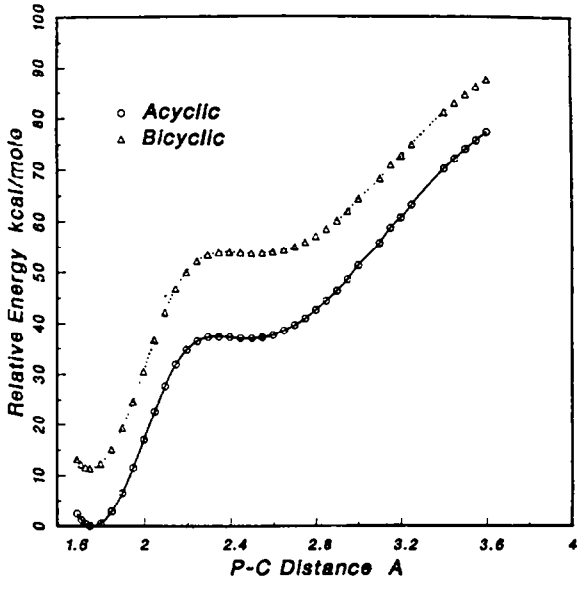

Fig. 3

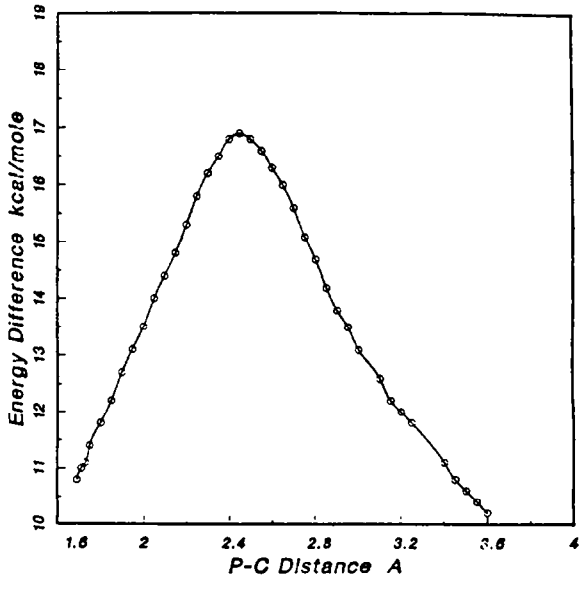

Fig. 4

Figure 3 Relative energy diagram for the decomposition of phosphoranes A1 and C1 (via pathway/search a; STO-3G basis set).

Figure 4 Energy difference between phosphoranes C1 and A1 as a function of P-C distance for reaction path shown in Figure 3.

are used as nucleophiles in place of $(EtO)_3P{=}O$. In our previous calculation a proton was the electrophile.[12] In both calculations the putative "transition state" with the bicyclic geometry is found to be much higher in energy than the acyclic transition state, rationalizing why the bicyclic phosphate cannot be alkylated.

The breakdown of the phosphoranes A1 and C1 with cleavage of the C-O bond may provide an explanation of the desulfurization process of the Corey-Winter olefin synthesis.[53-55]

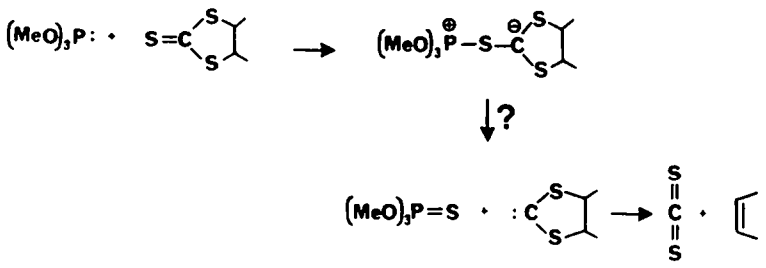

The mechanism of the Corey-Winter reaction is thought to involve initial thiophilic addition of the phosphorus to the thiocarbonyl group and α-elimination of the thionophosphate to yield a carbene. Trapping of the carbene trivalent phosphorus (trimethyl phosphite) yields an ylide, which subsequently fragments to the olefin, trimethyl thiophosphate and carbon disulfide. Addition of benzaldehyde suppresses olefin formation, instead, giving the ketene thioacetal. Carbene "dimer" is also obtained and these results have been used as arguments in favor of the intermediacy of the ylide, 1,3-dipole and/or carbene.

CONCLUSION

Search of the reaction hypersurface between phosphite and formaldehyde reveals a path involving formation of a phosphorane which has the carbon atom at an axial position of a distorted trigonal bipyramid. In the transition state, structures which have oxygen lone pairs app to the newly formed bond can stabilize the transition state. The kinetic stereoelectronic effect stabilization is presumably the result of two electron interaction between the app lone pair orbital and the the antibonding orbital of the newly forming bond.

A conformation maximizing these interactions has an activation energy 7 kcal/mol lower energy than a conformation without oxygen lone pairs app to the translating P-C bond.

The origin of the α-effect, the enhanced nucleophilicity of a base possessing a heteroatom with an adjacent unshared electron pair is suggested to arise from this kinetic stereoelectronic effect.

ACKNOWLEDGMENT. Support by NSF (CHEM 83k0098) and NIH (GM 36281) is acknowledged.

REFERENCES

1 Hudson, R. F., Verkade, J. G., **Tetrahedron Lett. 37**, 3231 (1975).

2 Verkade, J. G., **Bioinorg. Chem. 3**, 165 (1974).

3 Verkade, J. G., **Phosphorus Sulfur 2**, 251 (1976).

4 Hodges, R. V.; Houle, F. A.; Beaucham, J. L.; Montag, R. A.; Verkade, J. G., **J. Am. Chem. Soc. 102**, 932 (1980).

5 Vande Griend, L. J.; Verkade, J. G.; Pennings, J. F.; Buck, H. M., **J. Am. Chem. Soc. 99**, 2459 (1977).

6 Cowley, A. H.; Lattman, M.; Montag, R. A.; Verkade, J. G., **Inorg. Chim. Acta 25**, 151 (1977).

7 Westheimer, F. H., **Acc. Chem. Res. 1**, 70 (1968).

8 Zverev, V. V ; Villem, J.; Arshinova, R. P., **Dokl. Akad. Nauk. SSSR 256**, 1412 (1981).

9 Cowley, A. H.; Goodman, D. W.; Kuebler, N. A.; Sanchez, M.; Verkade, J. G., **Inorg. Chem. 16**, 854 (1977).

10 Yarbrough, L. W.; Hall, M. B., **J. Chem. Soc. Chem. Commun.**, 161 (1978).

11 Taira, K.; Mock, W.L.; Gorenstein, D. G., **J. Am. Chem. Soc. 106**, 7831 (1984).

12 Taira, K.; Gorenstein, D. G., **J. Am. Chem. Soc. 106**, 7825 (1984); Gorenstein, D. G.; Chang, A., and Yang, Ji-C., **Tetrahedron**, in press; Yang, J. C.; Gorenstein, D.G. **Tetrahedron**, in press.

13 Taira, K.; Gorenstein, D. G., **Tetrahedron 40**, 3215 (1984).

14 Taira, K.; Fanni, T.; Gorenstein, D. G., **J. Am. Chem. Soc. 106**, 1521 (1984); Taira, K.; Fanni, T., Gorenstein, D.G.: Vaidyanathaswamy; and Verkade, J. G., **J. Am. Chem. Soc. 108**, 6311 (1986).

15 Gorenstein, D. G.; Taira, K., **J. Am. Chem. Soc. 104**, 6130 (1982).

16 Deslongchamp, P., **Stereoelectronic Effects in Organic Chemistry**; Pergamon Press, Oxford (1983).

17 Kirby, A. J., **The Anomeric Effect and Related Stereoelectronic Effects at Oxygen**; Springer-Verlag, Berlin (1983).

18 Creary, Y; Mehrsheikh-Mohammadi, M.E., **J. Org. Chem. 51**, 7 (1986).

19 Gaussian 80: Binkley, J. A.; Whiteside, R. A.; Krishnan, R.; Seeger, R.; Defrees, D. J.; Schlegel, H. B.; Topiol, S.; Kahn, L. R.; Pople, J. A., **Gaussian 80: QCPE**, 13 437 (1981). Corrections by A. B. Buda, E. Osawa and T. D. Bouman.

20 Murtagh, B. A.; Sargent, R. W., **The Computer J. 13**, 185 (1970).

21 Johnson, C.K., **ORTEP: A Fortran Thermal-Ellipsoid Plot Program for Crystal Structure Illustrations**; Oak Ridge National Laboratory.

22 Gorenstein, D. G.; Westheimer, F. H., **J. Am. Chem. Soc. 89**, 2762 (1967).

23 Muetterties, E. L.; Schunn, R. A., **Quart. Rev. (London) 20**, 245 (1966).

24 Ramirez, F.; Madan, O. P., **J. Am. Chem. Soc. 87**, 731 (1965).

25 Schmutzler, R., **Angew. Chem. Intl. Ed. Engl. 4**, 496 (1965).

26 Gorenstein, D. G.; Westheimer, F. H., **J. Am. Chem. Soc. 92**, 634 (1970).

27 Gorenstein, D. G., **J. Am. Chem. Soc. 92**, 644 (1970).

28 Gorenstein, D. G.; Findlay, J. B.; Luxon, B. A.; Kar, D., **J. Am. Chem. Soc. 99**, 3473 (1977).

29 Gorenstein, D. G.; Luxon, B. A.; Findlay, J. B.; Momii, R., **J. Am. Chem. Soc. 99**, 4170 (1977).

30 Gorenstein, D. G.; Luxon, B. A.; Findlay, J. B., **J. Am. Chem. Soc. 99**, 8048 (1977).

31 Gorenstein, D. G.; Luxon, B. A.; Goldfield, E. M., **J. Am. Chem. Soc., 102**, 1757 (1980).

32 Gorenstein, D. G.; Rowell, R.; Taira, K., **ACS Symposium No. 171, Phosphorus Chemistry 69** (1981).

33 Bestman, H. J ; Chandrasekar, J.; Downey, W. G.; Schleyer, P. R., **J. Am. Chem. Soc. 102**, 978 (1980).

34 Deakyne, C. A.; Allen, L. C., **J. Am. Chem. Soc. 98**, 4076 (1976).

35 Hoffmann, R.; Howell, J. M.; Muetterties, E. L., **J. Am. Chem. Soc. 94**, 3047 (1972).

36 Howell, J. M., **J. Am. Chem. Soc. 97**, 3930 (1975).

37 Keil, F.; Kutzelnigg, W., **J. Am. Chem. Soc. 97**, 3623 (1975).

38 Strich, A.; Veillard, A., **J. Am. Chem. Soc. 95**, 5574 (1973).

39 Emsley, J.; Hall, D., **The Chemistry of Phosphorus**; Wiley, New York (1976).

40 Borden, W. T., **Modern Molecular Orbital Theory for Organic Chemists**; Prentice-Hall, New Jersey (1975).

41 Burgi, H. B.; Lehn, J. M.; Wipff, G., **J. Am. Chem. Soc. 96**, 1956 (1974).

42 Burgi, H. B.; Dunitz, J. D.; Lehn, J. M.; Wipff, G., **Tetrahedron 30**, 1563 (1974).

43 Baldwin, J. W., **J. Chem. Soc., Chem. Commun.**, 734 (1976).

44 Liotta, C. L.; Burgess, E. M.; Eberhardt, W. H., **J. Am. Chem. Soc. 106**, 4849 (1984).

45 Binkley, J. S.; Pople, J. A., **J. Chem. Phys. 64**, 5112 (1976).

46 DePuy, C. H.; Della, E. W.; Filley, J.; Grabowski, J. J.; Bierbaum, V. M., **J. Am. Chem. Soc. 105**, 2481 (1983).

47 Grekov, A. P.; Veselov, V. Y., **Russian Chem. Review 47**, 631 (1978).

48 Fina, N. J.; Edwards, J. O., **Int. J. Chem. Kinetics 5**, 1 (1973).

49 Filippini, F.; Hudson, R. F., **J. Chem. Soc. Chem. Commun.**, 522 (1972).

50 Hudson, R. F.; Filippini, F., **J. Chem. Soc., Chem. Commun.**, 726 (1972).

51 Klopman, G.; Evans, R. C., **Tetrahedron 34**, 269 (1978).

52 Heaton, M. M., **J. Am. Chem. Soc. 100**, 2004 (1978).

53 Corey, E. J.; Winter, J., **J. Am. Chem. Soc. 85**, 2677 (1963).

54 Corey, E. J., **Pure Appl. Chem. 14**, 19 (1967).

55 Block, E., **Reactions of Organosulfur Compounds**; Academic Press, New York, 229-235 (1978).